LANGMUIR

pubs.acs.org/Langmuir Article

In Situ Regeneration of Silicon Microring Biosensors Coated with Parylene C

Huan Zhang,[#] Xiaoqing Lv,[#] Beiju Huang,[*] Chuantong Cheng, Zan Zhang, Zanyun Zhang, Weihao Fang, Hengjie Zhang, Run Chen, Yulong Huang, and Hongda Chen

Cite This: *Langmuir* 2022, 38, 504−513 Read Online

ACCESS | Metrics & More | Article Recommendations

ABSTRACT: Optical biosensors support disease diagnostic applications, offering high accuracy and sensitivity due to label-free detection and their optical resonance enhancement. However, optical biosensors based on noble metal nanoparticles and precise micro-electromechanical system technology are costly, which is an obstacle for their applications. Here, we proposed a biosensor reuse method with nanoscale parylene C film, taking the silicon-on-insulator microring resonator biosensor as an example. Parylene C can efficiently adsorb antibody by one-step modification without any surface treatment, which simplifies the antibody modification process of sensors. Parylene C (20 nm thick) was successfully coated on the surface of the microring to modify anti-carcinoembryonic antigen (anti-CEA) and specifically detect CEA. After sensing, parylene C was successfully removed without damaging the sensing surface for the sensor reusing. The experimental results demonstrate that the sensing response did not change significantly after the sensor was reused more than five times, which verifies the repeatability and reliability of the reusable method by using parylene C. This framework can potentially reduce the cost of biosensors and promote their further applications.

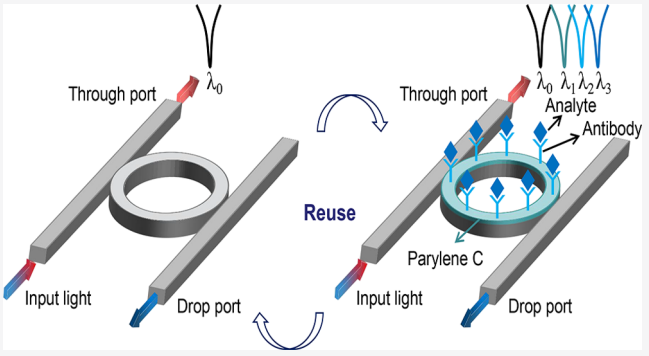

1. INTRODUCTION

Biomarker-based cancer diagnosis and treatment at the molecular level have recently emerged.[1] Biomarker detection sensors have a key role in the applications of liquid biopsy in terms of sensitivity and reliability.[2] Among these biosensors, there has been a great interest in optical biosensors because they offer high sensitivity for a wide range of biological analytes due to their optical resonance enhancement and label-free detection.[3] In addition, these biosensors are easy to prepare in small size by mature complementary metal-oxide-semiconductor (CMOS) technology, which enables the high-density heterogeneous integrated systems.

The performance of optical biosensors with high sensitivity depends on the fine nanostructure. Several groups have developed biosensors based on nanostructures with high sensitivity.[4−6] In some methods, Sreekanth et al. developed a miniaturized plasmonic biosensor based on a hyperbolic metamaterial using a grating coupling technique, which achieved ultralow-molecular-weight detection with an extreme sensitivity of 30,000 nm per refractive index unit (RIU).[4] Other biosensors based on nanostructures have been developed. Peng et al. designed a high-sensitivity refractive index biosensor, which is a one-dimensional photonic crystal cavity-coupled microring resonator (PCMRR).[5] The size and distribution of the nanostructures can be controlled to obtain high sensitivity. However, all these devices must be fabricated by electron beam lithography, ion beam lithography, and combining with other new materials, which is very expensive and has been one of the obstacles to their further applications. Thus, if the chip can be reusable, it will greatly reduce the cost of optical biosensors and promote their applications as the reuse method makes it possible to fabricate devices once but use them unlimited times. This is where our reuse approach is applied for.

The functional modification of the biosensor is an essential part to determine whether the chip can be reused. Covalent immobilization and physical adsorption are two of the most commonly modifications of chips. On one hand, covalent immobilization gives tight binding between the sensor surface and the specific antibodies or aptamers.[7] On the other hand, it requires a complex procedure, such as the mercaptan self-

Received: November 1, 2021
Revised: December 3, 2021
Published: December 29, 2021

https://doi.org/10.1021/acs.langmuir.1c02914
Langmuir 2022, 38, 504−513

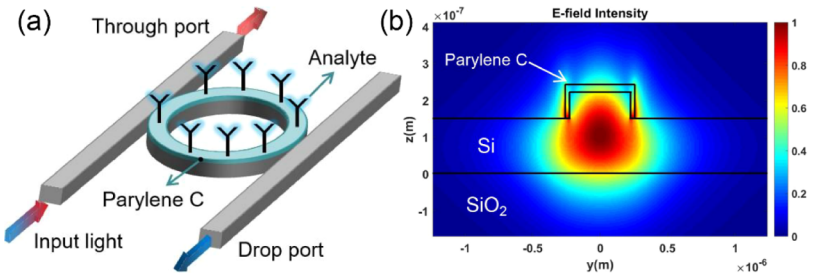

Figure 1. (a) Schematic diagram of the sensing microring of our work. (b) TE mode's E-field intensity of the ridge waveguide with 20 nm-thick parylene C.

assembly, which requires overnight modification and carboxyl activation.[8] Physical adsorption via ionic or van der Waals interactions is easier to handle and more time saving.[9] Several groups have developed methods of chip reusing.[10−13] In one method, chemical treatment was used to remove the residual antibodies, and new antibodies were applied for additional detection.[12,13] However, such a chemical treatment may contaminate the sensor surface and degrade the sensor performance, such as causing the loss of sensor signals.[14] A reusable magnetic surface plasmon resonance sensor chip that can repeatedly detect H1N1 virus was reported. A layer of magnetic particles trapped as a solid substrate was removed using external magnetic fields, and a new layer of magnetic particles was immobilized on the chip surface for additional sensing.[10] However, the introduction of magnetic fields increases the complexity of the sensing system. A simpler and more effective method to reuse optical biosensors needs to be developed.

Parylene C, which is a well-known polymer material with excellent chemical stability and high biocompatibility, usually functions as a passivation coating to achieve good barrier properties. Recent studies have shown various functions of parylene C, for example, as a medium between Si-PDMS and Si−Si bonding microfluidic chips,[15] as a material to fabricate flexible polymer devices,[16] and as cell separation filters.[17] However, there has been little research on using parylene C as a medium between the sensor surface and the antibody to modify the sensor and removing parylene C to reuse the sensor. Parylene C can efficiently adsorb antibody by one-step modification, which simplifies the antibody modification process of sensors. In addition, parylene C can grow on the surface of any material, which includes silicon,[18] gold,[19] silver,[20] silicon nitride,[21] SiON,[22] and so on. Because of the resistance of parylene C to indissolubility in almost all known organic solvents and inorganic reagents, it is particularly difficult to remove parylene C. However, there are several effective methods for the parylene C removal, including focused heat, plasma, and mechanical methods.[23] These advantages of parylene C enable it to be a medium for antibody modification and sensor reusing.

In this work, we have demonstrated that parylene C can be used as a medium for antibody modification on the sensor surface. Taking the silicon optical microring resonator biosensor as an example, we proposed a method to reuse optical biosensors by using parylene C. Parylene C with a thickness of 20 nm was successfully grown on the surface of the microring, and the antibody was immobilized on the surface of parylene C with high efficiency by one-step modification with no surface treatment, which simplified the antibody modification process of sensors. Using this method, carcinoembryonic antigen (CEA) was detected using the microring biosensor. In addition, we also studied and compared the effect of different removal methods of parylene C and successfully removed parylene C without damaging the sensing surface of the microring biosensor by using the tetrahydrofuran (THF)-submerged method. The results of five experiments demonstrated the repeatability and reliability of the reusable method by using parylene C.

2. MATERIALS AND METHODS

Silicon microrings have been a widely studied sensing method because of their high sensitivity, label-free detection, and highly compact integration. A schematic diagram of the sensing microring of our work is shown in Figure 1a, which includes a symmetric add-drop microring, a parylene C film, and analytes. The incident light propagating in the through waveguide is coupled into the ring, where light exists in the form of whispering gallery modes. During the light circulation in the ring, specific wavelengths of light result in resonance due to optical interference, which is defined by the resonance condition[24]

$$m\lambda = 2\pi R n_{\text{eff}} \tag{1}$$

where λ is the resonance wavelength, R is the ring radius, n_{eff} is the effective refractive index of the ring, and m is an integer. According to eq 1, the shift of the resonance wavelength depends on the change in n_{eff} due to the analytes, which is used for sensing in our work.

The microring is covered with parylene C, which adsorbs analytes by the surface immobilization mechanism of physisorption.[25] To further analyze the effect of parylene C and the analytes, the TE mode's E-field intensity of the 70 nm-high and 450 nm-wide ridge waveguide with 20 nm-thick parylene C was calculated in Lumerical MODE, as shown in Figure 1b. A strong E-field intensity distribution remained out of the area of parylene C, while most of the E-field intensities were bound in the core of the single-mode ridge waveguide. Assuming that the average height of the antibody was approximately 10 nm,[26] the interaction of the E-field intensity and antibody could be quantificationally represented using the power confinement factor Γ_t, which is defined as[27]

$$\Gamma_t = \frac{\iint_{\Omega t} E^* \times H dx dy}{\iint_{\Omega T} E^* \times H dx dy} \tag{2}$$

where Ωt is the antibody region, which is the area expanded outside parylene C, while ΩT is the entire cross-section of the waveguides. The power confinement factor Γ_t of the antibody is 1.22%, which indicates that the antibody has a large impact on the optical field of the sensing device.

For qualitative analysis of the sensing device based on the microring, the sensitivity of the microring was used to characterize the sensing performance, which was defined using the following expression[9]

$$S = \frac{\Delta\lambda}{\Delta n_{\text{clad}}} \tag{3}$$

https://doi.org/10.1021/acs.langmuir.1c02914
Langmuir 2022, 38, 504−513

where $\Delta\lambda$ is the resonance wavelength shift and Δn_{clad} is the change in refractive index of the cladding material, which is determined using the adhesive analytes on the functionalized surface of the microring. The unit of S is often written as nm/RIU.

3. RESULTS AND DISCUSSION

3.1. Device Fabrication. The device was fabricated on a silicon-on-insulator (SOI) wafer by standard CMOS technology. The optical microscope images and scanning electron microscopy (SEM) images of the sensor microring are shown in Figure 2, which consist of a grating coupler, a microring, and

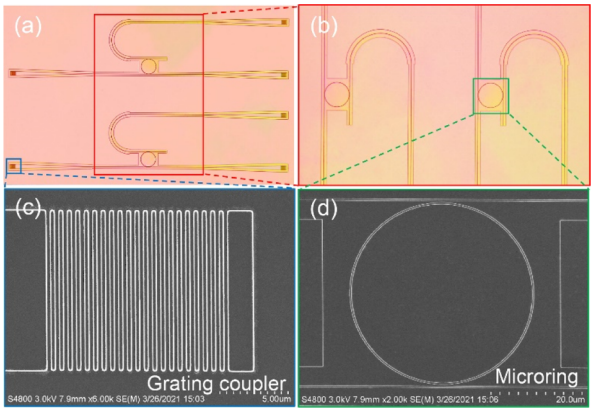

Figure 2. (a,b) Optical microscope images and (c,d) SEM images of the sensor microring.

a through and drop port. The gap between the through or drop port and the microring with a radius of 20 μm is approximately 250 nm, while the width of the 70 nm-etched ridge waveguide is approximately 450 nm. The process flow of the sensing experiment is shown in Figure 3. The first process step of the sample was the wet etching of the SiO_2 passivation layer to expose the surface of the waveguides. Then, the sample was cleaned and sequentially soaked in acetone, ethyl alcohol, and deionized water. Parylene C was grown by chemical vapor deposition with a specialty coating system (Model PDS 2010). Afterward, antibody and antigen sensing was proceeded. Finally, the parylene C film was removed after sensing, and the procedure proceeded to the next round of sensing. The entire process of parylene C growth, functionalization, and parylene C removal was repeated, which indicated the repeatability and reliability of our reusable sensors.

3.2. Sensing. To verify the functionality and performance of the sensing device based on the microring with parylene C, a simulation analysis was performed to determine the relationship between the resonance wavelength shift and the refractive index in Lumerical MODE Solutions. The thickness of the ridge waveguide was 70 nm and the gap between the through or drop port and the microring was 250 nm, which coincided with those of the above fabricated ones. The thickness and refractive index of parylene C were approximately 20 nm and 1.639, respectively. The absorption was negligible because the material exhibited very little absorption in the C-band and L-band and the film was very thin. The normalized transmission of the sensing microring without and with parylene C is shown in Figure 4a. The dotted lines refer to the sensing microring without parylene C while the solid lines refer to that with parylene C. The resonance wavelength evidently red-shifted to the right when the refractive index changed from 1.33 to 1.39, regardless of whether the devices were with parylene C, which is indicated using eq 1. In addition, the resonance wavelengths with parylene C are on the right side of those without parylene C because the refractive index of parylene C is larger than that of air. The relationship of the resonance wavelength shift versus the refractive index without and with parylene C is shown using the black and red solid lines with symbols in Figure 4b, respectively. Sensitivity S of the sensing microring without and with parylene C was 42.8 and 38.7 nm/RIU, respectively, which indicates that the parylene film only has little impact on the sensitivity of the microring. The reason is that the parylene film slightly weakens the interaction of the analyte with the evanescent field, resulting from their separation at a certain distance with respect to the thickness. In summary, the device based on the microring with parylene C is a good alternative candidate for sensing.

To obtain better sensing performance, the film was optimized to have the minimal thickness in the preliminary experiment, which was reduced from 44.097 to 20.990 nm as measured by atomic force microscopy (AFM) and shown in

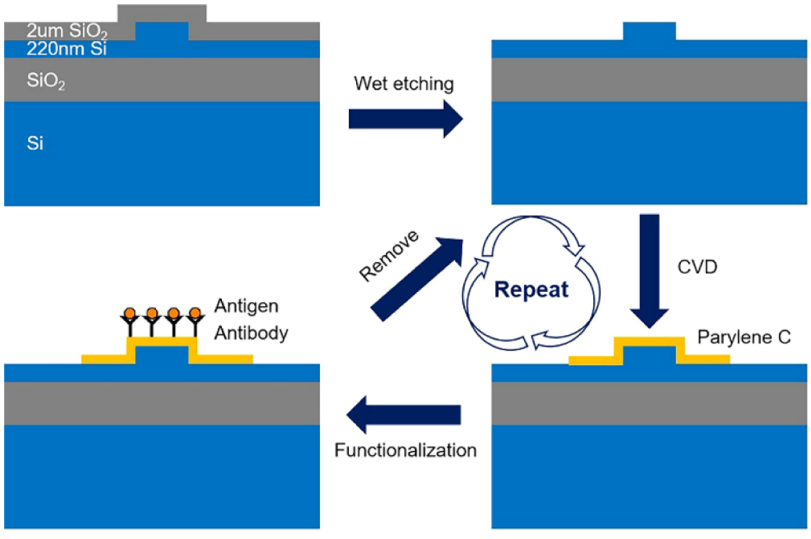

Figure 3. Process flow of the sensing experiment.

https://doi.org/10.1021/acs.langmuir.1c02914
Langmuir 2022, 38, 504−513

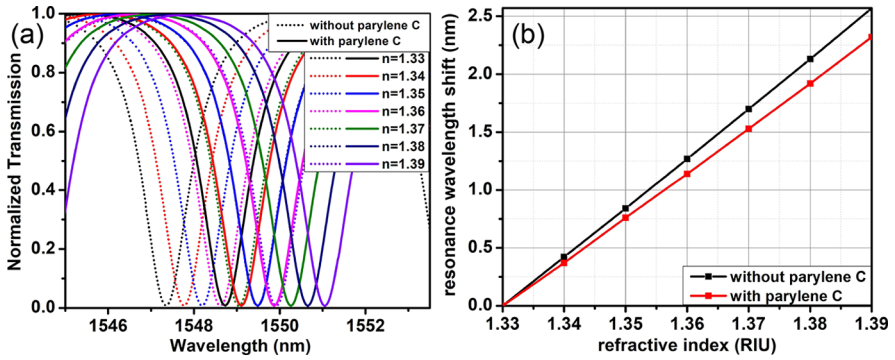

Figure 4. (a) Normalized transmission of the sensing microring without and with parylene C. (b) Resonance wavelength shift versus refractive index change without and with parylene C.

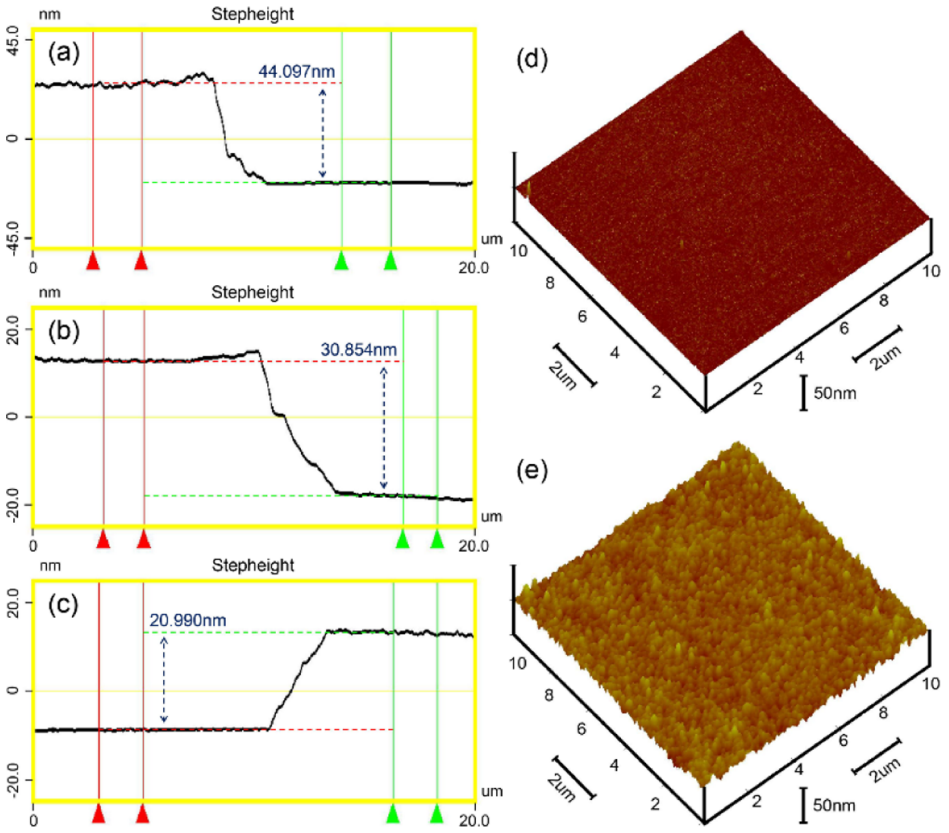

Figure 5. (a–c) Optimization of the thickness of the parylene C film measured by AFM. (d,e) Surface roughness of the sample without and with the parylene C film. The imaging region is a 10 × 10 μm square.

Figure 5a–c. The defects of the parylene C film significantly increased when the thickness was less than 20 nm. As a result, the efficiency of antibody modification on the film decreased. In addition, the surface roughness values of the samples without and with parylene C were 0.426 and 3.134 nm, respectively, as shown in Figure 5d,e. The surface roughness increased by 7.36 times, which signifies that the parylene C film increased the contact area of the upper surface with the analyte, which is beneficial to sensing.

There are many ways of antibody adsorption on the surface of the solid substrate, including physical adsorption and chemical bond multilayer self-assembly. Hydrophilic absorption and hydrophobic absorption both belong to physical absorption. Some research studies use hydrophilic interaction such as the situation in ref 28. The hydrophilic modification of parylene C facilitates the adsorption of chemical factors, thus improving cell adhesion efficiency. Others rely on the interaction of hydrophobic groups between the solid substrate and antibody, which is similar to the way of antibody coating on the poly(propylene) substrate of ELISA. Parylene C is hydrophobic, which may allow a strong hydrophobic force between the antibody and solid substrate.

To identify the adsorption capacity of parylene C, different types of materials were assessed by using the Alexa Fluor 488 antibody (Thermo Fisher Scientific, USA) as a signal, which was a kind of antibody directly conjugated with Alexa Fluor 488 fluorescence/dye. The fluorescent antibody was added to the materials at a concentration of 10 μg/mL. After 1 h, photographs were taken under a fluorescent microscope. Figure 6 shows different adsorption capabilities of parylene C,

https://doi.org/10.1021/acs.langmuir.1c02914
Langmuir 2022, 38, 504–513

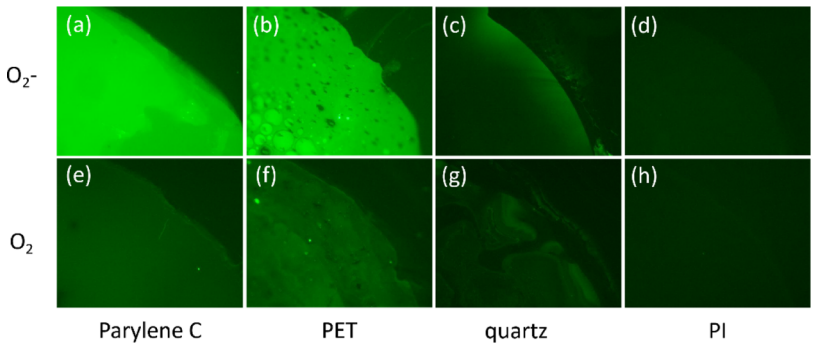

Figure 6. Physical adsorption capability of different materials. (a,e) Parylene C, (b,d) PET, (c,g) quartz, and (d,h) PI; (a−d) without plasma treatment and (e−h) with plasma treatment.

PET, quartz, PI, several common materials for physical adsorption. Figure 6a−d shows that the fluorescence intensity gradually decreased, which indicates the stronger antibody adsorption capacity of parylene C. It has been demonstrated that the plasma-treated parylene N film had high protein-immobilization efficiency.[29] Thus, different plasma treatment times were assessed in the experiment. Figure 6a−d shows the no-plasma-treated experiment, while Figure 6e−h shows the plasma-treated experiment. This result indicated that the plasma treatment can make the material surface hydrophilic. Physical adsorption relies on hydrophobic bonding. Adhesion is enhanced on hydrophobic surfaces.[30] Antibody modification was set as a direct addition, which saved time and simplified the experiment compared with plasma treatment. Hence, parylene C can efficiently adsorb antibody by one-step modification without any surface treatment.

Then, parylene C was grown on the microring. After the growth of a parylene C film with 20 nm thickness, the fluorescent antibody was added on the surface of the sensors at a concentration of 10 μg/mL for 1 h. The samples were washed with 1× phosphate-buffered saline (PBS) buffer (Beijing Solarbio Science and Technology Co., Ltd) before microscope photography. Figure 7a shows a micrograph of the parylene C film after being modified with a fluorescent antibody. Figure 7b shows the fluorescent field of Figure 7a, which indicates that the Alexa Fluor 488 antibody was successfully modified on the parylene C film by physical adsorption. After the antibody absorption ability of parylene C had been tested, parylene C was removed. A photomicrograph of the microring without parylene C is shown in Figure 7c. The color of the region coated with parylene C differed from that without parylene C. Figure 7d shows the fluorescent field of Figure 7c, which indicates that the fluorescence of the Alexa Fluor 488 antibody disappeared when the parylene C film was removed.

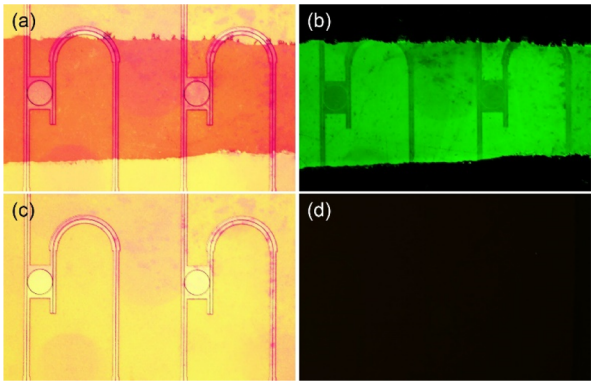

Figure 7. Micrograph of microrings with antibody modification before and after parylene removal. (a,b) Alex Fluor 488 antibody was modified on the parylene C film: (a) bright field and (b) fluorescent field. (c,d) Microring after the removal of the parylene C film: (c) bright field and (d) fluorescent field.

Furthermore, the biomarker detection performance and the specificity of the microring with parylene C was assessed. To show the response of the sensor to their target analyte with and without the deposited antibody, 1% bovine serum albumin (BSA) (Beijing Solarbio Science and Technology Co., Ltd) was added to the parylene C film followed by 1 μg/mL carcinoma embryonic antigen (CEA) (Fitzgerald Industries International, USA). The normalized transmission of the microring during the sensing experiment is shown in Figure 8a. The black and red curves represent the spectrum of the microring before and after coated with parylene C, while the blue and green curves represent the spectrum after modification on the parylene C film with 1% BSA and adding CEA. The result showed that there was no response after CEA was added to the sensor without anti-carcinoembryonic antigen (anti-CEA) (Fitzgerald Industries International, USA). Then, the specificity of the sensor was also tested. After growing parylene C, the microring was modified with anti-CEA at a concentration of 10 μg/mL in PBS buffer containing 1% BSA. Then, 1 μg/mL CEA was added on the surface of the sensor and washed with 1× PBS buffer. Meanwhile, 1 μg/mL IgG (Beijing Solarbio Science and Technology Co., Ltd) was detected after anti-CEA was added with the same treatment as the experimental control group. The normalized transmission of the microring was obtained and is shown in Figure 8b,c. The result showed that the spectrum of CEA had a redshift of 0.24 nm compared with that of anti-CEA while there was no spectral shift between anti-CEA and IgG. It proved the specificity of the deposited antibody to the analyte. To evaluate the sensor response in more complex solutions, CEA in serum was detected and the result is shown in Figure 8d. The spectrum of CEA in serum had a redshift of 0.24 nm compared with that of anti-CEA, which indicated that the sensor could response in complex solutions. In summary, the sensor had a good sensing performance of detecting the analytes.

3.3. Parylene C Removal. Considering the excellent chemical stability of parylene C, oxygen-based plasma, boiling in piranha solution (H_2SO_4/H_2O_2 = 7:3), and submerging in THF solvent are used for the parylene C removal. For the oxygen-based plasma method, parylene C is removed by

https://doi.org/10.1021/acs.langmuir.1c02914
Langmuir 2022, 38, 504−513

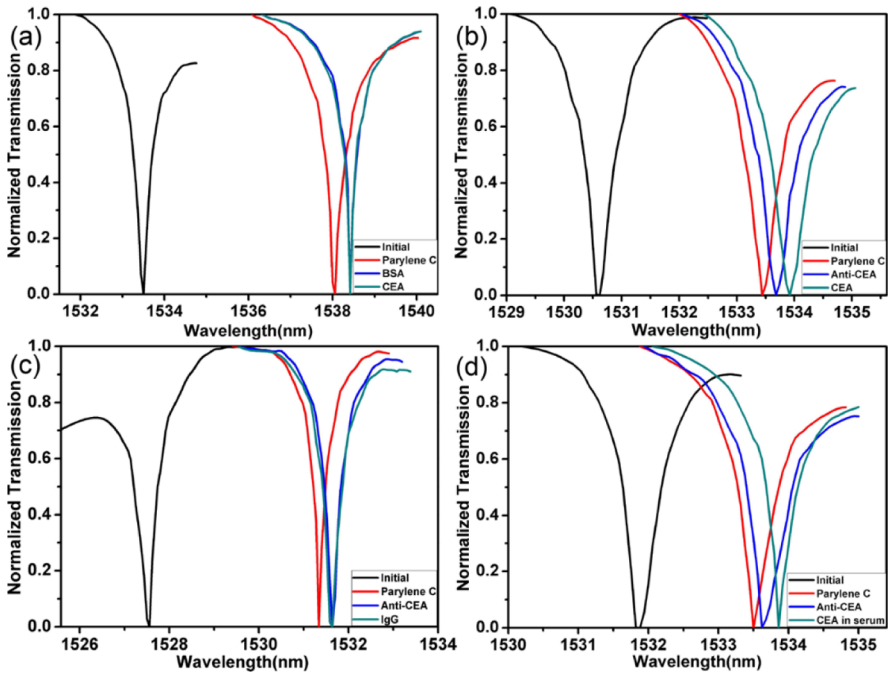

Figure 8. Normalized transmission of the microring during the sensing experiment. (a) 1% BSA and CEA. (b) Anti-CEA and CEA. (c) Anti-CEA and IgG. (d) Anti-CEA and CEA in serum.

opening the benzene ring of the substance, which introduces an oxygen radical and subsequently generates a hydroxyl radical between benzene rings in the polymer chain. Afterward, a peroxy radical is generated by the absorption of oxygen and rearranged to carbon monoxide or dioxide gas, which will escape from the surface of the sample.[31] The condition of plasma removal in our experiment was approximately 1.5 L/min oxygen flow for 120 s with 120 W of forward power and 4 W of reflected power. With respect to the other two methods, the main difference was the processing temperature. For the method of boiling in piranha solution, the sample was boiled at 250 °C for half an hour. The method of submerging in THF solvent was operated at room temperature for 36 h; then, the film was softened and loosened from the substrate surface by using 90% power ultrasonic cleaning in ethyl alcohol for 20 min.

The normalized transmission of the samples processed by the three methods is shown in Figure 9a–c. The plasma-treated resonance wavelength was non-coincident and exhibited a 0.36 nm blueshift compared with the initial wavelength. The reason may be that the substrate surface was damaged by the oxygen-based plasma, which led to the smaller effective refractive index of the microring. For the method of boiling in the piranha solution, the treated resonance wavelength was red-shifted by 0.36 nm to the initial wavelength, which may result from the intermediate derivative generated during the boiling process. The THF-treated resonance wavelength coincided with the initial resonance wavelength, which indicates that the substrate surface was fully protected without damage, and there were no generated intermediate derivatives during removal. For further analysis, the surface roughness of the samples processed by the three methods is shown in Figure 9d–f using AFM, which were 0.168, 4.362, and 0.406 nm for the plasma-treated, H_2SO_4-boiled, and THF-submerged methods, respectively. Thus, the THF-submerged surface had the most similar roughness to the primitive surface (0.426 nm), while that of the other two methods deviated from the primitive value, which implies that the THF-submerged method can obtain a lossless surface.

3.4. Repeatability and Reliability. Because the THF solvent removes parylene C from the substrate surface without damage, repeating the sensing process several times is of great importance to verify the reliability of the repeatability. The wavelength shifts during the whole sensing process, after growing parylene C, sensing antibody, and removing parylene C are shown in Figure 10, which were the results of five repetition cycles. The wavelength shifts of the sensing antibody were basically constant, near 0.3 nm, although those of the device with parylene C fluctuated up and down, which indicates that the thickness of the parylene C film was not uniform in these repetition cycles but had no impact on the sensing process. The thickness uniformity of the parylene C film is determined by the vacuum and temperature of the deposition process,[32] which are necessary to optimize in the following work. For the wavelength shift after parylene C removal, it maybe results from the temperature jitter during the measurement process because of the thermo-optic effect. Meanwhile, the minimum detection wavelength of the spectrometer was approximately 0.06 nm, which led to a worse result. In addition, a few materials might remain in the slit between the microring and the through or drop port. However, the sensing process eliminated the influence of the deviation of the wavelength shift, which originated from the nonuniform thickness of parylene C or parylene C removal. It is necessary to note that the main purpose of the repetition experiments is to demonstrate that during the whole sensing process, the microring can work well and its structure is not damaged. It will be our next work to design a highly sensitive microring structure to do control experiments for nonspecific binding or cross-reactive binding and the sensitivity of the device to protein.

https://doi.org/10.1021/acs.langmuir.1c02914
Langmuir 2022, 38, 504–513

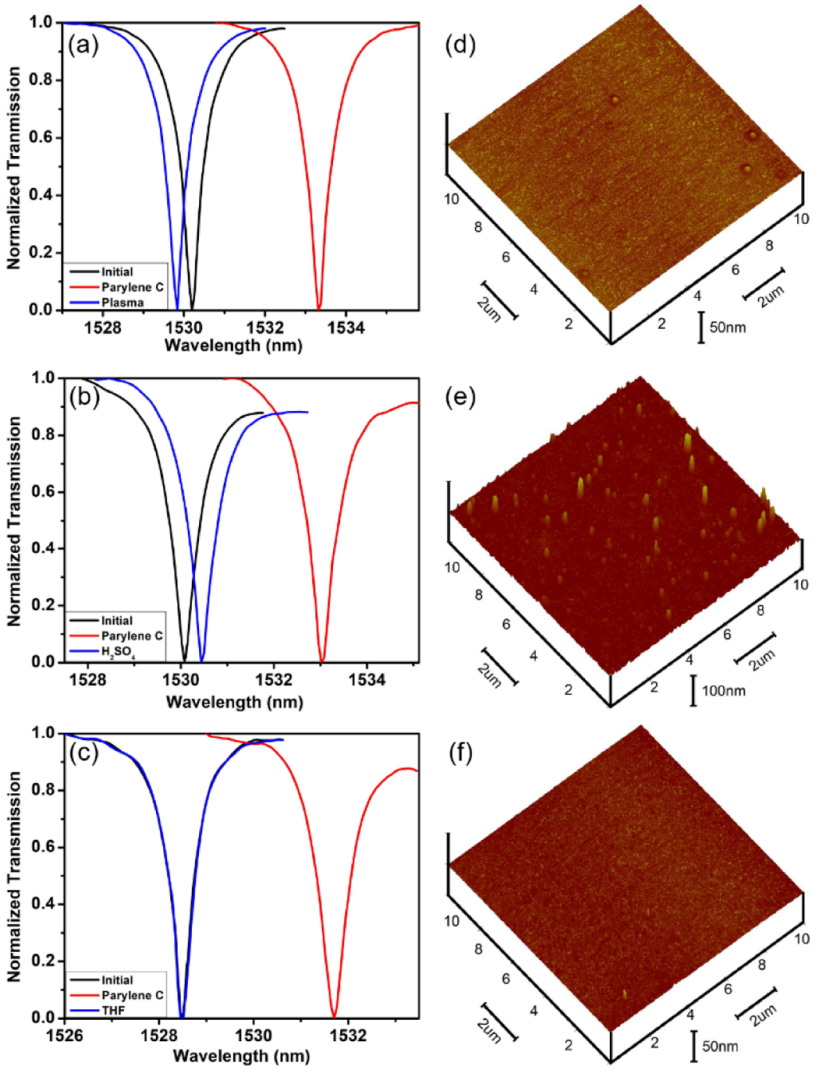

Figure 9. (a–c) Normalized transmission of the samples processed by the three methods. (d–f) Surface roughness of the samples processed by the three methods. The imaging region is a 10 × 10 μm square.

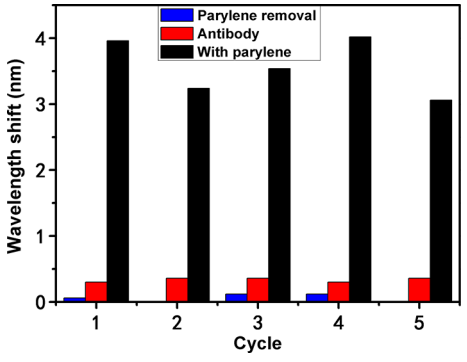

Figure 10. Wavelength shifts during the whole sensing process, after growing parylene C, sensing antibody, and removing parylene C.

There will be a lot of difficulties to solve and a long way to go to apply our reuse method in the field of industrialization for mass production. However, it is of great use for some laboratory research studies in the early exploration and a lot of tests in the market, which involve sampling customers and bring samples to manufacturer's laboratories, where the sensor is recovered and reused. Besides, our reuse method will make point-of-care and personalized medicine affordable for everyone because of low cost caused by the reuse method in the future.

Compared to other biosensing techniques, the main advantages of microring resonators are their small size, scalable mass production, and the possibility for portable devices for point-of-care applications.[9] To further improve the sensing performance, some effort can be made in terms of the device structure and materials. For the device structure, the microdisk[33,34] and microsphere resonators[35,36] can replace the microring resonators for sensing, whose larger Q factors are beneficial to sense ultralow analyte concentrations and lead to higher sensing sensitivity. In addition, many studies have demonstrated that slot waveguides[37] or microrings based on slot waveguides[38] can be used for sensing because they can enhance the interaction between light and matter, which makes high sensitivity possible. Besides, for the device materials, the Si_3N_4 material is utilized to fabricate the ultrahigh-Q microcavities to enhance the sensing sensitivity.[39]

Because the microring sensing device is compatible with universal CMOS processes, it is suitable to be integrated with microfluidic channels to realize a microfluidic control chip to sense small-volume and low-concentration liquid analytes.[40]

https://doi.org/10.1021/acs.langmuir.1c02914
Langmuir 2022, 38, 504–513

For microfluidic chip biosensors, there are two methods of coating parylene C: (1) Parylene C is only coated at sensing hotspots of the substrate, but not in areas where the substrate and microchannel bonds are, using a mask. (2) Parylene C is coated on the whole substrate, and then, microchannels are bonded with assembly jig. In addition, by incorporating microring and fiber arrays, it is possible to build a high-throughput and integrated lab-on-a-chip experimental platform.[41,42]

Protein adsorption on solid surfaces is a complicated process, which has been discussed in a review.[43] Finding an easy-to-operate and high-adsorption antibody modification method is essential in the application of sensors, which is beneficial for improving the efficiency and reducing costs. Parylene C has a strong antibody adsorption ability without plasma treatment, whereas parylene N and parylene A have the opposite effects.[44] Parylene C can be grown on the surface of many materials, which indicates the universality of the method. Thus, the proposed sensor reuse method here can be used in optical biosensors and electrochemical-based and acoustic-based biosensors. Furthermore, our method may have applications in the field of implantable sensors because of the biocompatibility, corrosion resistance, and stability of parylene C.[45]

4. CONCLUSIONS

To decrease the cost and achieve the reuse of biosensors, a surface regeneration technique for SOI microring resonators was proposed in this paper, which targeted parylene C-based reusable biosensors. Parylene C can efficiently adsorb antibody by one-step modification without any surface treatment compared with other common materials for physical adsorption. This one-step antibody coupling method can simplify the antibody modification process of sensors. By coating with a 20 nm-thick layer of parylene C on the surface of the microring biosensor, anti-CEA was easily modified on the sensor and CEA was successfully detected. Meanwhile, parylene C can be easily removed without damaging the sensing surface to reuse the sensors. The experimental results showed a good repeatable sensing ability after the sensor was reused more than five times, which further proved the repeatability and reliability of the method by using parylene C. This framework can potentially reduce the cost of biosensors and promote their further applications.

AUTHOR INFORMATION

Corresponding Author

Beiju Huang − *State Key Laboratory on Integrated Optoelelctronics, Institute of Semiconductors, Chinese Academy of Sciences, Beijing 100083, China; College of Materials Science and Opto-Electronic Technology, University of Chinese Academy of Sciences, Beijing 100049, China; Beijing Key Laboratory of Inorganic Stretchable and Flexible Information Technology, Beijing 100083, China;* orcid.org/0000-0002-6902-6554; Email: bjhuang@semi.ac.cn

Authors

Huan Zhang − *State Key Laboratory on Integrated Optoelelctronics, Institute of Semiconductors, Chinese Academy of Sciences, Beijing 100083, China; College of Materials Science and Opto-Electronic Technology, University of Chinese Academy of Sciences, Beijing 100049, China*

Xiaoqing Lv − *State Key Laboratory on Integrated Optoelelctronics, Institute of Semiconductors, Chinese Academy of Sciences, Beijing 100083, China; College of Materials Science and Opto-Electronic Technology, University of Chinese Academy of Sciences, Beijing 100049, China*

Chuantong Cheng − *State Key Laboratory on Integrated Optoelelctronics, Institute of Semiconductors, Chinese Academy of Sciences, Beijing 100083, China; College of Materials Science and Opto-Electronic Technology, University of Chinese Academy of Sciences, Beijing 100049, China;* orcid.org/0000-0002-6130-5524

Zan Zhang − *School of Electronic and Control Engineering, Chang'an University, Xi'an 710064, China*

Zanyun Zhang − *School of Electronical and Electronic Engineering, Tiangong University, Tianjin 300387, China*

Weihao Fang − *State Key Laboratory on Integrated Optoelelctronics, Institute of Semiconductors, Chinese Academy of Sciences, Beijing 100083, China; College of Materials Science and Opto-Electronic Technology, University of Chinese Academy of Sciences, Beijing 100049, China*

Hengjie Zhang − *State Key Laboratory on Integrated Optoelelctronics, Institute of Semiconductors, Chinese Academy of Sciences, Beijing 100083, China; College of Materials Science and Opto-Electronic Technology, University of Chinese Academy of Sciences, Beijing 100049, China*

Run Chen − *State Key Laboratory on Integrated Optoelelctronics, Institute of Semiconductors, Chinese Academy of Sciences, Beijing 100083, China; College of Materials Science and Opto-Electronic Technology, University of Chinese Academy of Sciences, Beijing 100049, China*

Yulong Huang − *State Key Laboratory on Integrated Optoelelctronics, Institute of Semiconductors, Chinese Academy of Sciences, Beijing 100083, China; College of Materials Science and Opto-Electronic Technology, University of Chinese Academy of Sciences, Beijing 100049, China*

Hongda Chen − *State Key Laboratory on Integrated Optoelelctronics, Institute of Semiconductors, Chinese Academy of Sciences, Beijing 100083, China; College of Materials Science and Opto-Electronic Technology, University of Chinese Academy of Sciences, Beijing 100049, China; Beijing Key Laboratory of Inorganic Stretchable and Flexible Information Technology, Beijing 100083, China*

Complete contact information is available at: https://pubs.acs.org/10.1021/acs.langmuir.1c02914

Author Contributions

#H.Z. and X.L. contributed equally to this paper.

Notes

The authors declare no competing financial interest.

ACKNOWLEDGMENTS

This work was supported by the National Key R&D Program of China (grant no. 2018YFA0209000), the National Natural Science Foundation of China (grant nos. 61974099, 62022081, 61634006, and 62004192), and the Youth Innovation Promotion Association of Chinese Academy of Sciences (grant no. 2018146).

REFERENCES

(1) Chi, K. R. The Tumour Trail Left in Blood. *Nature* **2016**, *532*, 269−271.

(2) Alharthi, S. D.; Bijukumar, D.; Prasad, S.; Khan, A. M.; Mathew, M. T. Evolution in Biosensors for Cancers Biomarkers Detection: A Review. *J. Bio. Tribo. Corrosion* **2021**, *7*, 42.
(3) Soler, M.; Lechuga, L. M. Principles, Technologies, and Applications of Plasmonic Biosensors. *J. Appl. Phys.* **2021**, *129*, 111102.
(4) Sreekanth, K. V.; Alapan, Y.; ElKabbash, M.; Ilker, E.; Hinczewski, M.; Gurkan, U. A.; De Luca, A.; Strangi, G. Extreme Sensitivity Biosensing Platform Based on Hyperbolic Metamaterials. *Nat. Mater.* **2016**, *15*, 621−627.
(5) Peng, F.; Wang, Z.; Guan, L.; Yuan, G.; Peng, Z. High-Sensitivity Refractive Index Sensing Based on Fano Resonances in a Photonic Crystal Cavity-Coupled Microring Resonator. *IEEE Photonics J.* **2018**, *10*, 1.
(6) Yavas, O.; Aćimović, S. S.; Garcia-Guirado, J.; Berthelot, J.; Dobosz, P.; Sanz, V.; Quidant, R. Self-Calibrating On-Chip Localized Surface Plasmon Resonance Sensing for Quantitative and Multiplexed Detection of Cancer Markers in Human Serum. *ACS Sens.* **2018**, *3*, 1376−1384.
(7) Washburn, A. L.; Gunn, L. C.; Bailey, R. C. Label-Free Quantitation of a Cancer Biomarker in Complex Media Using Silicon Photonic Microring Resonators. *Anal. Chem.* **2009**, *81*, 9499−9506.
(8) Vashist, S. K.; Lam, E.; Hrapovic, S.; Male, K. B.; Luong, J. H. T. Immobilization of Antibodies and Enzymes on 3-Aminopropyltriethoxysilane-Functionalized Bioanalytical Platforms for Biosensors and Diagnostics. *Chem. Rev.* **2014**, *114*, 11083−11130.
(9) Steglich, P.; Hülsemann, M.; Dietzel, B.; Mai, A. Optical Biosensors Based on Silicon-On-Insulator Ring Resonators: A Review. *Molecules* **2019**, *24*, 519.
(10) Yoo, H.; Shin, J.; Sim, J.; Cho, H.; Hong, S. Reusable Surface Plasmon Resonance Biosensor Chip for the Detection of H1N1 Influenza Virus. *Biosens. Bioelectron.* **2020**, *168*, 112561.
(11) Geng, X.; Zhang, M.; Long, H.; Hu, Z.; Zhao, B.; Feng, L.; Du, J. A Reusable Neurotransmitter Aptasensor for the Sensitive Detection of Serotonin. *Anal. Chim. Acta* **2021**, *1145*, 124−131.
(12) Hsu, H.-F.; Lin, Y.-T.; Huang, Y.-T.; Lu, M.-F.; Chen, C.-H. In Situ Regeneration of Si-Based ARROW-B Surface Plasmon Resonance Biosensors. *J. Med. Biol. Eng.* **2015**, *35*, 305−314.
(13) Feng, X.; Zhang, G.; Chin, L. K.; Liu, A. Q.; Liedberg, B. Highly Sensitive, Label-Free Detection of 2,4-Dichlorophenoxyacetic Acid Using an Optofluidic Chip. *ACS Sens.* **2017**, *2*, 955−960.
(14) Goode, J. A.; Rushworth, J. V. H.; Millner, P. A. Biosensor Regeneration: A Review of Common Techniques and Outcomes. *Langmuir* **2015**, *31*, 6267−6276.
(15) Ciftlik, A. T.; Dupouy, D. G.; Gijs, M. A. M. Programmable Parylene-C Bonding Layer Fluorescence for Storing Information on Microfluidic Chips. *Lab Chip* **2013**, *13*, 1482.
(16) Lin, M.; Chen, Q.; Wang, Z.; Fang, Y.; Liu, J.; Yang, Y.; Wang, W.; Cai, Y.; Huang, R. Flexible Polymer Device Based on Parylene-C with Memory and Temperature Sensing Functionalities. *Polymers* **2017**, *9*, 310.
(17) Liu, Y.; Xu, H.; Dai, W.; Li, H.; Wang, W. 2.5-Dimensional Parylene C Micropore Array with a Large Area and a High Porosity for High-Throughput Particle and Cell Separation. *Microsyst. Nanoeng.* **2018**, *4*, 13.
(18) Mudumba, S.; de Alba, S.; Romero, R.; Cherwien, C.; Wu, A.; Wang, J.; Gleeson, M. A.; Iqbal, M.; Burlingame, R. W. Photonic Ring Resonance Is a Versatile Platform for Performing Multiplex Immunoassays in Real Time. *J. Immunol. Methods* **2017**, *448*, 34−43.
(19) Figueiredo, N. M.; Serra, R.; Cavaleiro, A. Robust LSPR Sensing Using Thermally Embedded Au Nanoparticles in Glass Substrates. *Nanomaterials* **2021**, *11*, 1592.
(20) Priya, S.; Laha, R.; Dantham, V. R. Wavelength-Dependent Angular Shift and Figure of Merit of Silver-Based Surface Plasmon Resonance Biosensor. *Sens. Actuators, A* **2020**, *315*, 112289.
(21) Wörhoff, K.; Heideman, R. G.; Leinse, A.; Hoekman, M. TriPleX: A Versatile Dielectric Photonic Platform. *Adv. Opt. Technol.* **2015**, *4*, 189−207.
(22) Samusenko, A.; Gandolfi, D.; Pucker, G.; Chalyan, T.; Guider, R.; Ghulinyan, M.; Pavesi, L. A SiON Microring Resonator-Based Platform for Biosensing at 850 Nm. *J. Lightwave Technol.* **2016**, *34*, 969−977.
(23) Callahan, R. R. A.; Pruden, K. G.; Raupp, G. B.; Beaudoin, S. P. Downstream Oxygen Etching Characteristics of Polymers from the Parylene Family. *J. Vac. Sci. Technol., B* **2003**, *21*, 1496.
(24) Baehr-Jones, T.; Hochberg, M.; Walker, C.; Eric Chan, E.; Koshinz, D.; Krug, W.; Scherer, A. Analysis of the Tuning Sensitivity of Silicon-on-Insulator Optical Ring Resonators. *J. Lightwave Technol.* **2005**, *23*, 4215−4221.
(25) Pereiro, I.; Cors, J. F.; Pané, S.; Nelson, B. J.; Kaigala, G. V. Underpinning Transport Phenomena for the Patterning of Biomolecules. *Chem. Soc. Rev.* **2019**, *48*, 1236−1254.
(26) Jo, S.; Lee, W.; Park, J.; Kim, W.; Kim, W.; Lee, G.; Lee, H.-J.; Hong, J.; Park, J. Localized Surface Plasmon Resonance Aptasensor for the Highly Sensitive Direct Detection of Cortisol in Human Saliva. *Sensor. Actuator. B Chem.* **2020**, *304*, 127424.
(27) Zhang, H.; Huang, B.; Zhang, Z.; Cheng, C.; Zhang, Z.; Zhang, H.; Chen, R.; Chen, H. On-Chip Photonic Synapses Based on Slot-Ridge Waveguides With PCMs For In-Memory Computing. *IEEE Photonics J.* **2021**, *13*, 1−13.
(28) Trantidou, T.; Rao, C.; Barrett, H.; Camelliti, P.; Pinto, K.; Yacoub, M. H.; Athanasiou, T.; Toumazou, C.; Terracciano, C. M.; Prodromakis, T. Selective Hydrophilic Modification of Parylene C Films: A New Approach to Cell Micro-Patterning for Synthetic Biology Applications. *Biofabrication* **2014**, *6*, 025004.
(29) Choi, Y.-H.; Lee, G.-Y.; Ko, H.; Chang, Y. W.; Kang, M.-J.; Pyun, J.-C. Development of SPR Biosensor for the Detection of Human Hepatitis B Virus Using Plasma-Treated Parylene-N Film. *Biosens. Bioelectron.* **2014**, *56*, 286−294.
(30) Sethuraman, A.; Han, M.; Kane, R. S.; Belfort, G. Effect of Surface Wettability on the Adhesion of Proteins. *Langmuir* **2004**, *20*, 7779−7788.
(31) Meng, E.; Li, P.-Y.; Tai, Y.-C. Plasma Removal of Parylene C. *J. Micromech. Microeng.* **2008**, *18*, 045004.
(32) Herrera-Alonso, M.; McCarthy, T. J. Chemical Surface Modification of Poly(p-Xylylene) Thin Films. *Langmuir* **2004**, *20*, 9184−9189.
(33) Krioukov, E.; Klunder, D. J. W.; Driessen, A.; Greve, J.; Otto, C. Sensor Based on an Integrated Optical Microcavity. *Opt. Lett.* **2002**, *27*, 512.
(34) Boyd, R. W.; Heebner, J. E. Sensitive Disk Resonator Photonic Biosensor. *Appl. Opt.* **2001**, *40*, 5742.
(35) Vollmer, F.; Braun, D.; Libchaber, A.; Khoshsima, M.; Teraoka, I.; Arnold, S. Protein Detection by Optical Shift of a Resonant Microcavity. *Appl. Phys. Lett.* **2002**, *80*, 4057−4059.
(36) Gorodetsky, M. L.; Savchenkov, A. A.; Ilchenko, V. S. Ultimate Q of Optical Microsphere Resonators. *Opt. Lett.* **1996**, *21*, 453.
(37) Barrios, C. A. Optical Slot-Waveguide Based Biochemical Sensors. *Sensors* **2009**, *9*, 4751−4765.
(38) Claes, T.; Molera, J. G.; De Vos, K.; Schacht, E.; Baets, R.; Bienstman, P. Label-Free Biosensing With a Slot-Waveguide-Based Ring Resonator in Silicon on Insulator. *IEEE Photonics J.* **2009**, *1*, 197−204.
(39) Barclay, P. E.; Srinivasan, K.; Painter, O.; Lev, B.; Mabuchi, H. Integration of Fiber-Coupled High-Q SiNx Microdisks with Atom Chips. *Appl. Phys. Lett.* **2006**, *89*, 131108.
(40) Geidel, S.; Llopis, S. P.; Rodrigo, M.; de Diego-Castilla, G.; Sousa, A.; Nestler, J.; Otto, T.; Gessner, T.; Parro, V. Integration of an Optical Ring Resonator Biosensor into a Self-Contained Microfluidic Cartridge with Active, Single-Shot Micropumps. *Micromachines* **2016**, *7*, 153.
(41) De Vos, K.; Bartolozzi, I.; Schacht, E.; Bienstman, P.; Baets, R. Silicon-on-Insulator Microring Resonator for Sensitive and Label-Free Biosensing. *Opt. Express* **2007**, *15*, 7610.
(42) Ramachandran, A.; Wang, S.; Clarke, J.; Ja, S. J.; Goad, D.; Wald, L.; Flood, E. M.; Knobbe, E.; Hryniewicz, J. V.; Chu, S. T.; Gill, D.; Chen, W.; King, O.; Little, B. E. A Universal Biosensing Platform

Based on Optical Micro-Ring Resonators. *Biosens. Bioelectron.* **2008**, *23*, 939−944.
(43) Rabe, M.; Verdes, D.; Seeger, S. Understanding Protein Adsorption Phenomena at Solid Surfaces. *Adv. Colloid Interface Sci.* **2011**, *162*, 87−106.
(44) Park, K.; Kim, J. Y.; Pyun, G.Y. Parylene-Coated Polytetrafluoroethylene-Membrane-Based Portable Urea Sensor for Real-Time Monitoring of Urea in Peritoneal Dialysate. *Sensors* **2019**, *19*, 4560.
(45) Kuo, W.-C.; Wu, T.-C.; Wu, C.-F.; Wang, W.-C. Bioperformance Analysis of Parylene C Coating for Implanted Nickel Titanium Alloy. *Mater. Today Commun.* **2021**, *27*, 102306.

https://doi.org/10.1021/acs.langmuir.1c02914
Langmuir 2022, 38, 504−513